

Transport spin current driven by the moving kink crystal in a chiral helimagnet

I. G. Bostrem,¹ Jun-ichiro Kishine,² and A. S. Ovchinnikov¹

¹Department of Physics, Ural State University, Ekaterinburg, 620083 Russia

²Faculty of Engineering, Kyushu Institute of Technology, Kitakyushu 804-8550, Japan

(Received 17 January 2008; revised manuscript received 13 March 2008; published 11 April 2008)

We show that the bulk transport magnetic current is generated by the moving magnetic kink crystal (chiral soliton lattice) formed in the chiral helimagnet under the static magnetic field applied perpendicular to the helical axis. The current is caused by the nonequilibrium transport momentum with the kink mass being determined by the spin fluctuations around the kink crystal state. An emergence of the transport magnetic currents is then a consequence of the dynamical off-diagonal long range order along the helical axis. We derive an explicit formula for the inertial mass of the kink crystal and the current in the weak field limit.

DOI: [10.1103/PhysRevB.77.132405](https://doi.org/10.1103/PhysRevB.77.132405)

PACS number(s): 72.25.-b, 05.45.Yv, 75.47.-m, 85.75.-d

How to create, transport, and manipulate spin currents is a central problem in the multidisciplinary field of spintronics.¹ The key theoretical concepts there include the current-driven spin-transfer torque² and resultant force acting on a domain wall³ (DW) in metallic ferromagnetic/nonmagnetic multilayers, the dissipationless spin currents in paramagnetic spin-orbit coupled systems,⁴ and magnon transport in textured magnetic structures.⁵ A fundamental query behind the issue is how to describe transport magnetic currents.⁶ Conventionally, the charge current is defined by the product of the carrier density and the drift velocity related via the continuity equation. In the case of spin current, the deviation of the spin projection from its equilibrium value plays a role of a charge. Then, an emergence of the transport magnetic currents may be expected in nonequilibrium state as a manifestation of the dynamical off-diagonal long range order (ODLRO).⁷ Historically, Döring⁸ first pointed out that the longitudinal component of the slanted magnetic moment inside the Bloch DW emerges as a consequence of translational motion of the DW. An additional magnetic energy associated with the resultant demagnetization field is interpreted as the kinetic energy of the wall.

Recent progress of material synthesis sheds new light on this problem. In a series of magnets belonging to chiral space group without any rotoinversion symmetry elements, the crystallographic chirality gives rise to the asymmetric Dzyaloshinskii interaction that stabilizes either left-handed or right-handed chiral magnetic structures.⁹ In these chiral helimagnets, magnetic field applied perpendicular to the helical axis stabilizes a periodic array of DWs with definite spin chirality forming kink crystal or chiral soliton lattice.¹⁰ In this Brief Report, we demonstrate that the magnetic transport analogous to Döring effect⁸ occurs in the moving kink crystal of chiral helimagnets and serves an example of the dynamical ODLRO in nonequilibrium state. An essential point is that the kink crystal state has a degeneracy originating from the translational symmetry. Consequently, the transport momentum has a form $M\dot{X}$, where M and X represent the kink mass and the collective coordinate of the kink in the laboratory frame. The kink crystal behaves as a heavy object with the inertial mass M .

We start with a spin Hamiltonian describing the chiral helimagnet,

$$\mathcal{H} = -J \sum_{\langle i,j \rangle} \mathbf{S}_i \cdot \mathbf{S}_j + \mathbf{D} \cdot \sum_{\langle i,j \rangle} \mathbf{S}_i \times \mathbf{S}_j - \tilde{\mathbf{H}} \cdot \sum_i \mathbf{S}_i, \quad (1)$$

where the first term represents the ferromagnetic coupling with the strength $J > 0$ between the nearest neighbor $\mathbf{S}_i = S(\cos \theta_i, \sin \theta_i \cos \varphi_i, \sin \theta_i \sin \varphi_i)$ and \mathbf{S}_j , where θ_i and φ_i denote the local polar coordinates. The second term represents the parity-violating Dzyaloshinskii interaction restricted to the nearest neighbor pairs of the adjacent ferromagnetic planes, which are characterized by the monoaxial vector $\mathbf{D} = D\hat{\mathbf{e}}_x$ along a certain crystallographic chiral axis (taken as the x axis). The third term represents the Zeeman coupling with the magnetic field $\tilde{\mathbf{H}} = 2\mu_B H \hat{\mathbf{e}}_y$ applied *perpendicular* to the chiral axis. When $H = 0$, the long-period incommensurate helimagnetic structure is stabilized with the definite chirality (left handed or right handed) fixed by the direction of the monoaxial \mathbf{D} vector.

In the continuum limit, the Hamiltonian density corresponding to the lattice Hamiltonian (1) is written as

$$\mathcal{H} = \frac{1}{2} (\partial_x \theta)^2 + \frac{1}{2} \sin^2 \theta (\partial_x \varphi)^2 - q_0 \sin^2 \theta (\partial_x \varphi) - \beta \sin \theta \cos \varphi, \quad (2)$$

where the energy is measured by JS^2 and $\beta = \tilde{H}/JS$. The semiclassical spin variable is represented as $\mathbf{S} = S(\cos \theta, \sin \theta \cos \varphi, \sin \theta \sin \varphi)$ by using the slowly varying polar angles $\theta(x)$ and $\varphi(x)$ [see Fig. 1(a)]. The helical pitch for the zero field ($\beta = 0$) is given by $q_0 = \tan^{-1}(D/J) \approx D/J$. Under the transverse field, a regular array of the magnetic kink is formed.¹¹ The kink corresponds to the phase

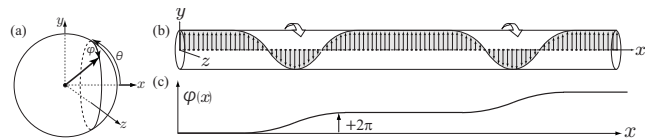


FIG. 1. (a) Polar coordinates in the laboratory frame. (b) Formation of the magnetic kink crystal in the chiral helimagnets under the transverse magnetic field, and (c) concomitant phase modulation. In (b), we depict a linear array of the spins along one chiral axis that is ferromagnetically coupled to the neighboring arrays.

winding in the left-handed ($\Delta\varphi=+2\pi$) or right-handed ($\Delta\varphi=-2\pi$) manners. Since we assume the uniform monoaxial Dzyaloshinskii vector \mathbf{D} , the kink with only positive (left-handed) or negative (right-handed) charge are energetically favored. The kink with the same charge repel each other, just like in the case of the Coulomb repulsion. So, the magnetic kink crystal (soliton lattice) is formed, as shown in Figs. 1(b) and 1(c).

The magnetic kink crystal phase is described by the stationary soliton solution, $\theta=\pi/2$ and $\cos[\varphi_0(x)/2]=\text{sn}(mx/\kappa)$, where $m=\sqrt{\beta}$ corresponds to the first breather mass and “sn” denotes a Jacobian elliptic function.¹¹ The period of the kink crystal is given by $l_0=2\kappa K(\kappa)/\sqrt{\beta}$. The elliptic modulus κ ($0<\kappa<1$) is determined by the energy minimization condition $E(\kappa)/\kappa=\pi q_0/4m$. Here, $K(\kappa)$ and $E(\kappa)$ denote the elliptic integrals of the first and second kinds, respectively.

Now, we consider the fluctuations around the classical solution and write $\theta(x)=\pi/2+u(x)$ and $\varphi(x)=\varphi_0(x)+v(x)$. When we consider only the tangential φ mode, our problem is reduced to the one first investigated by Sutherland.¹² The φ mode is fully studied in the context of the chiral helimagnet.^{13,14} In the present work, however, it is essential to take into account not only the φ mode but the θ mode to argue the longitudinal magnetic current. Expanding Eq. (2) up to u^2 and v^2 , we have $H=\int dx(\mathcal{H}_0+\mathcal{H}_u+\mathcal{H}_v+\mathcal{H}_{\text{int}})$, where \mathcal{H}_0 gives the classical solution and $\mathcal{H}_u=u\mathcal{L}_u u$ and $\mathcal{H}_v=v\mathcal{L}_v v$, where the differential operators are defined by

$$\mathcal{L}_u = -\frac{1}{2}\partial_x^2 - \frac{1}{2}(\partial_x\varphi_0)^2 + q_0(\partial_x\varphi_0) + \frac{1}{2}\beta \cos \varphi_0, \quad (3)$$

$$\mathcal{L}_v = -\frac{1}{2}\partial_x^2 + \frac{1}{2}\beta \cos \varphi_0. \quad (4)$$

The lowest-order coupling between the u and v modes comes from $\mathcal{H}_{\text{int}}=-u^2(\partial_x v)^2/2$, which is neglected here. In the case of zero field, $\beta=0$, we have $\mathcal{L}_u=-\partial_x^2/2+q_0^2/2$ and $\mathcal{L}_v=-\partial_x^2/2$. Therefore, we see that u mode acquires the mass q_0 (scaled by JS^2), while the v mode becomes massless. This situation naturally arises because the v mode is a Goldstone mode, but the u mode is not. Even after switching the perpendicular field, the u mode (v mode) remains to be massive (massless).

From now on, we argue that the massive θ fluctuations carry the magnetic current. First, we perform the mode expansions, $v(x,t)=\sum_n \eta_n(t)v_n(x)$ and $u(x,t)=\sum_n \xi_n(t)u_n(x)$, and seek the energy dispersions for the normal vibrational modes, satisfying $\mathcal{L}_u u_n(x)=\lambda_n u_n(x)$ and $\mathcal{L}_v v_n(x)=\rho_n v_n(x)$, respectively. Introducing $\tilde{x}=mx/\kappa$, we have the Schrödinger equations,

$$d^2 u_n(x)/d\tilde{x}^2 = [2\kappa^2 \text{sn}^2 \tilde{x} - \kappa^2(1 + 2\lambda_n/\beta) - 4 + 4\kappa\tau]u_n(x), \quad (5)$$

$$d^2 v_n(x)/d\tilde{x}^2 = [2\kappa^2 \text{sn}^2 \tilde{x} - \kappa^2(1 + 2\rho_n/\beta)]v_n(x), \quad (6)$$

with $\tau=q_0/m$. In Eq. (5), we consider the case of weak field corresponding to small κ , leading to $\text{dn } x \approx 1$. Now, Eqs. (5) and (6) reduce to the Jacobi form of the Lamé equation,¹⁵

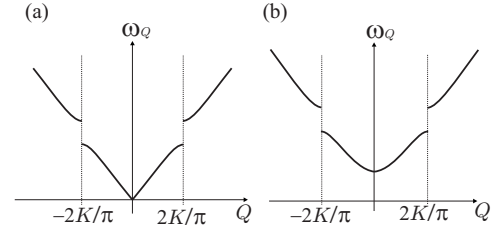


FIG. 2. The energy dispersions of the eigen modes for (a) the tangential φ fluctuation ($\omega_Q=\sqrt{\rho}$) and (b) the longitudinal θ -fluctuations ($\omega_Q=\sqrt{\lambda}$).

$d^2\Lambda_\alpha(x)/dx^2=\{\ell(\ell+1)\kappa^2 \text{sn}^2 x+A\}\Lambda_\alpha(x)$, with $\ell=1$. It is known that the solution is parametrized by a single continuous complex parameter α as^{12,13}

$$\Lambda_\alpha(x) = N \frac{\vartheta_4[\pi(x-x_0)/2K]}{\vartheta_4(\pi x/2K)} e^{-iQx}, \quad (7)$$

where N is a normalizing factor and ϑ_i ($i=1,2,3,4$) denote the theta functions,¹⁵ with Q being the Floquet index.¹²⁻¹⁴ The energy dispersion is obtained by determining $A=-\kappa^2(1+\tilde{A})$ as a function of the Floquet index Q , which marks eigenstates instead of n . It is known¹² that the dispersion consists of two (generally $\ell+1$) bands specified by the acoustic branch $\tilde{A}_1=\kappa'^2/\kappa^2 \text{sn}^2(\alpha,\kappa')$, $Q_1=\pi\alpha/2KK'+Z(\alpha,\kappa')$, and the optical branch $\tilde{A}_2=1/[\kappa^2 \text{sn}^2(\alpha,\kappa')]$, $Q_2=\pi\alpha/2KK'+Z(\alpha,\kappa')+\text{dn}(\alpha,\kappa')\text{cn}(\alpha,\kappa')/\text{sn}(\alpha,\kappa')$, where $\alpha\in(-K',K')$. Here, K' denotes the elliptic integral of the first kind with the complementary modulus $\kappa'=\sqrt{1-\kappa^2}$ and Z denotes the zeta function.¹⁵ The complex parameter x_0 in Eq. (7) are given by $i\alpha+K$ and $i\alpha$ for the acoustic and optical branches, respectively. We have the acoustic branch, $0\leq\tilde{A}_1<\kappa'^2/2\kappa^2$ for $0\leq|Q_1|\leq\pi/2K$, and the optical branch, $1/\kappa^2\leq\tilde{A}_2<\infty$ for $\pi/2K\leq|Q_2|$. The energy gap $\Delta=1$, opens at $|Q|=\pi/2K$. We present the dispersions ω_Q in Fig. 2, where the gapless acoustic $\sqrt{\mu_B H S \tilde{A}_1^{1/2}}$ and optical $\sqrt{\mu_B H S \tilde{A}_2^{1/2}}$ bands of φ excitations are depicted together with the gapfull acoustic $\sqrt{\mu_B H S [\tilde{A}_1+4\tau/\kappa-4/\kappa^2]^{1/2}}$ and optical $\sqrt{\mu_B H S [\tilde{A}_2+4\tau/\kappa-4/\kappa^2]^{1/2}}$ bands of θ excitations.

Next, we consider the collective dynamics of the kink crystal. For this purpose, we carry out the canonical formulation by using the collective coordinate method.¹⁶ We start with the corresponding Lagrangian,

$$L = \int dx [S(1 - \cos \theta)\dot{\varphi}_t - \mathcal{V}(\theta, \varphi)], \quad (8)$$

where the Berry phase term is taken into account. The mode expansion leads to the vibrational term, $\mathcal{V}[\theta, \varphi]=\sum_n \lambda_n \xi_n^2 + \sum_n \rho_n \eta_n^2$. Elevating the position of the kink center X to a dynamical variable, we write the solution in the form

$$\varphi = \varphi_0[x - X(t)] + \sum_{n=1}^{\infty} \eta_n(t)v_n[x - X(t)],$$

$$\theta = \pi/2 + \sum_{n=1}^{\infty} \xi_n(t) u_n[x - X(t)]. \quad (9)$$

Plugging these expressions into the Lagrangian (8), we have $L = -S \sum_n \dot{\eta}_n(t) K_{1n} + S \dot{X} \sum_n K_{2n} \xi_n(t) - S \sum_{n,m} K_{3nm} \xi_n(t) \dot{\eta}_m(t) - \sum_n \lambda_n \xi_n^2 - \sum_n \rho_n \eta_n^2$, with the coefficients $K_{1n} = \int dx v_n(x)$, $K_{2n} = \int dx (\partial \varphi_0 / \partial x) u_n(x)$, and $K_{3nm} = \int dx u_m(x) v_n(x)$. This Lagrangian is *singular* because the determinant of the matrix of second derivatives of the Lagrangian with respect to velocities (Hessian) turns out to be zero. Therefore, we need to construct the Hamiltonian by using Dirac's prescription for the constrained Hamiltonian systems. The canonical momenta conjugated to the coordinates X , ξ_n , and η_n , i.e., $p_1 = \partial L / \partial \dot{X} = S \sum_n K_{2n} \xi_n$, $p_{2n} = \partial L / \partial \dot{\xi}_n = 0$, and $p_{3n} = \partial L / \partial \dot{\eta}_n = -S K_{1n} - S \sum_m K_{3nm} \xi_m$, lead to the extended Hamiltonian, $H^* = p_1 \dot{X} + \sum_n p_{2n} \dot{\xi}_n + \sum_n p_{3n} \dot{\eta}_n - L$ with a set of primary constraints,

$$\begin{aligned} \Phi_1^{(1)} &= p_1 - S \sum_n K_{2n} \xi_n = 0, \\ \Phi_{2n}^{(1)} &= p_{2n} = 0, \\ \Phi_{3n}^{(1)} &= p_{3n} + S K_{1n} + S \sum_m K_{3nm} \xi_m = 0. \end{aligned} \quad (10)$$

Because of a lack of primary expressible velocities, the Hamiltonian with the imposed constraints,

$$H^{(1)} = \Phi_1^{(1)} \dot{X} + \sum_n \Phi_{2n}^{(1)} \dot{\xi}_n + \sum_n \Phi_{3n}^{(1)} \dot{\eta}_n + H_{ph},$$

coincides with H^* , where $H_{ph} = \sum_n \lambda_n \xi_n^2 + \sum_n \rho_n \eta_n^2$. It governs the equations of motion of the constrained system, i.e., the constraints are hold at all times. This leads to a set of dynamical equations,

$$\begin{aligned} \sum_n K_{2n} \dot{\xi}_n &= 0, \\ -2\lambda_n \xi_n + \dot{X} S K_{2n} - S \sum_m K_{3nm} \dot{\eta}_m &= 0, \\ -2\rho_n \eta_n + S \sum_m K_{3nm} \dot{\xi}_m &= 0, \end{aligned} \quad (11)$$

to give $\dot{\xi}_n = 0$ and $\dot{\eta}_n = 0$. Imposing the secondary constraints $\Phi_n^{(2)} = \eta_n = 0$ to be constant in time, we obtain $\dot{\eta}_n = 0$. Together with the second constraint in Eq. (11), this yields $\xi_n = (S K_{2n} / 2\lambda_n) \dot{X}$, and we reach the final form of the physical Hamiltonian, $H_{ph} = p_1^2 / 2M$, where $p_1 = M \dot{X}$ involves the soliton mass

$$M = S^2 \sum_n \frac{K_{2n}^2}{2\lambda_n}. \quad (12)$$

Now, we are ready to define the longitudinal spin current. We start with the linear momentum carried by the kink crystal,

$$P = S \int_0^{L_0} (1 - \cos \theta) \varphi_x dx, \quad (13)$$

where L_0 is the system size. By using $\theta = \pi/2 + u$ and $\varphi = \varphi_0$ for a steady current, we obtain

$$\begin{aligned} P &\approx S[\varphi_0(L_0) - \varphi_0(0)] + S \int_0^{L_0} u(x) \frac{\partial \varphi_0}{\partial x} dx \\ &= 2\pi Q S + S \sum_n \xi_n K_{2n}. \end{aligned} \quad (14)$$

We here introduced the topological charge, $Q = [\varphi_0(L) - \varphi_0(0)] / 2\pi$. By using the result $\xi_n = (S K_{2n} / 2\lambda_n) \dot{X}$ and Eq. (12), we obtain an important formula,

$$P = 2\pi S Q + M \dot{X}, \quad (15)$$

that plays an essential role in this paper. The first term is associated with the equilibrium background momentum and the second one corresponds to the transport current carried by the θ fluctuations. Apparently, the transverse magnetic field increases a period of the kink crystal lattice and diminishes the topological charge Q , and therefore, it affects only the background linear momentum. The physical momentum related with a mass transport due to the excitations around the kink crystal state is generated by the steady movement.

The "superfluid mass current" is accompanied by the "superfluid magnetic current" transferred by the θ fluctuations. It is determined through the definition of the magnetic density,⁷ $\mathcal{N} = S(1 - \cos \theta)$. By using $\theta = \pi/2 + u(x, t)$, we have $\partial \mathcal{N} / \partial t = S \sin \theta \partial \theta / \partial t \approx S \partial u / \partial t$, with $u(x, t) = \sum_n \xi_n(t) u_n[x - X(t)]$. Therefore, for a steady current, we obtain the continuity equation

$$\frac{\partial \mathcal{N}}{\partial t} = -\dot{X}^2 \frac{\partial}{\partial x} \left(\sum_n \frac{S^2 K_{2n}}{2\lambda_n} u_n \right) = -\frac{\partial j^x}{\partial x}, \quad (16)$$

where we introduced the magnon time-even current carried by the θ fluctuations,

$$j^x = S^2 \dot{X}^2 \sum_n \frac{K_{2n}}{2\lambda_n} u_n. \quad (17)$$

Here, we used the fact $\dot{\xi}_n = 0$ because of the constraint. The time evenness is manifested by appearance of not \dot{X} but \dot{X}^2 . The important point to note is that *the only massive θ mode can carry the longitudinal magnon current as a manifestation of ordering in nonequilibrium state, i.e., dynamical off-diagonal long range order.*

The final stage is to explicitly compute Eq. (17). We can exactly prove that the optical branch does not contribute to the magnetic current because of the orthogonality (the proof is detailed in a later paper). After a lengthy but straightforward manipulation, the contribution of the acoustic branch is obtained as a function of $\tilde{x} = mx / \kappa$,

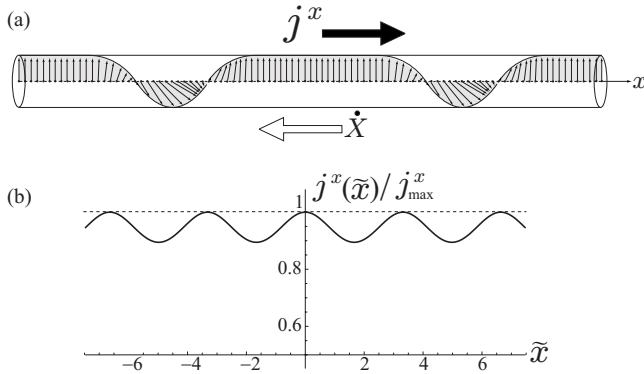


FIG. 3. (a) A schematic view of an instant distribution of spins in the current-carrying state. This picture corresponds to the case of intermediate field strength. (b) A snapshot of the position dependence of the current density $j^x(\tilde{x})$ in the weak field limit, which is exactly treated in this paper. $j^x(\tilde{x})$ is scaled by its maximum $j^x_{\max} = j^x(0)$.

$$j^x(\tilde{x}) = \frac{8E^2(\kappa)\dot{X}^2}{J\pi^2q_0^2[4E(\kappa)/\pi - 1]} \text{dn}(\tilde{x}) \approx \frac{2\dot{X}^2}{Jq_0^2} \text{dn}(\tilde{x}) \quad (18)$$

for the weak field case corresponding to small κ leading to $E(\kappa) \approx \pi/2$. On the other hand, the background spin current¹⁷ is shown to become $j_{\text{bg}}(x) \approx \partial\varphi_0(x)/\partial x - q_0 \propto \text{dn}(\tilde{x}) - 2E(\kappa)/\pi$. We stress that the physical meaning of j_{bg} is completely different from the current described by Eq. (18) in nonequilibrium state.¹⁸ We present a schematic view of an instant distribution of spins in the current-carrying state in Fig. 3(a). In Fig. 3(b), we present a snapshot of the position dependence of the current density $j^x(\tilde{x})$ in the weak field limit, which is given by Eq. (18).

In realizing the bulk magnetic current proposed here, a

single crystal of chiral magnets serves as spintronics device. The mechanism involves no spin-orbit coupling and the effect is not hindered by dephasing. Finally, we propose possible experimental methods to trigger off the spin current considered here. *Spin torque mechanism*: the spin-polarized electric current can exert torque to ferromagnetic moments through direct transfer of spin angular momentum.² This effect, which is related with Aharonov–Stern effect³ for a classical motion of magnetic moment in an inhomogeneous magnetic field, is eligible to excite the sliding motion of the kink crystal by injecting the spin-polarized current (polarized electron beam) in the direction either perpendicular or oblique to the chiral axis. The spin current transported by the soliton lattice may amplify the spin current of the injected carriers. *X-ray magnetic circular dichroism (XMCD)*: to detect the longitudinal magnetic currents accompanied by the dynamical ODLRO, XMCD may be used. Photon angular momentum may be aligned either parallel or antiparallel to the direction of the longitudinal net magnetization. *Ultrasound*: further possibility to control and detect the spin current is using a coupling between spins and chiral torsion.¹⁹ Ultrasound with the wavelength being adjusted to the period of the kink crystal may excite the periodic chiral torsion and resonantly supply the kinetic energy to the kink crystal. Consequently, the ultrasound attenuation may occur.²⁰ *Time of-flight (TOF) technique*: the most direct way of detecting the traveling magnon density may be winding a sample by a pickup coil and performing the TOF experiment. Then, the coil should detect a periodic signal induced by the magnetic current.

We acknowledge helpful discussions with Yu. A. Izyumov, K. Inoue, I. Fomin, and M. Sigrist. J.K. acknowledges Grant-in-Aid for Scientific Research (A) (No. 18205023) and (C) (No. 19540371) from the Ministry of Education, Culture, Sports, Science and Technology, Japan.

¹I. Žutić, J. Fabian, and S. Das. Sarma, *Rev. Mod. Phys.* **76**, 323 (2004) and references therein.

²J. C. Slonczewski, *J. Magn. Magn. Mater.* **159**, L1 (1996); L. Berger, *Phys. Rev. B* **54**, 9353 (1996); M. D. Stiles and A. Zangwill, *J. Appl. Phys.* **91**, 6812 (2002); *Phys. Rev. B* **66**, 014407 (2002); G. Tatara and H. Kohno, *Phys. Rev. Lett.* **92**, 086601 (2004).

³Y. Aharonov and A. Stern, *Phys. Rev. Lett.* **69**, 3593 (1992); Ya. B. Bazaliy, B. A. Jones, and S.-C. Zhang, *Phys. Rev. B* **57**, R3213 (1998); M. D. Stiles and A. Zangwill, *ibid.* **66**, 014407 (2002).

⁴E. I. Rashba, *Sov. Phys. Solid State* **2**, 1109 (1960); S. Murakami, N. Nagaosa, and S. C. Zhang, *Science* **301**, 1348 (2003); J. Sinova, D. Culcer, Q. Niu, N. A. Sinitsyn, T. Jungwirth, and A. H. MacDonald, *Phys. Rev. Lett.* **92**, 126603 (2004).

⁵P. Bruno and V. K. Dugaev, *Phys. Rev. B* **72**, 241302(R) (2005).

⁶E. I. Rashba, *J. Supercond.* **18**, 137 (2005).

⁷I. A. Fomin, *Physica B* **169**, 153 (1991); G. E. Volovik, arXiv:cond-mat/0701180 (unpublished).

⁸W. Döring, *Z. Naturforsch. A* **3a**, 374 (1948).

⁹I. E. Dzyaloshinskii, *J. Phys. Chem. Solids* **4**, 241 (1958).

¹⁰J. Kishine, K. Inoue, and Y. Yoshida, *Prog. Theor. Phys. Suppl.* **159**, 82 (2005).

¹¹I. E. Dzyaloshinskii, *Sov. Phys. JETP* **19**, 960 (1964); **20**, 665 (1965).

¹²B. Sutherland, *Phys. Rev. A* **8**, 2514 (1973).

¹³Yu. A. Izyumov and V. M. Laptev, *JETP Lett.* **62**, 755 (1985).

¹⁴D. N. Aristov and A. Luther, *Phys. Rev. B* **65**, 165412 (2002).

¹⁵E. T. Whittaker and G. N. Watson, *A Course of Modern Analysis* (Cambridge University Press, New York, 1927).

¹⁶N. H. Christ and T. D. Lee, *Phys. Rev. D* **12**, 1606 (1975).

¹⁷J. Heurich, J. König, and A. H. MacDonald, *Phys. Rev. B* **68**, 064406 (2003).

¹⁸J. Xiao, A. Zangwill, and M. D. Stiles, *Phys. Rev. B* **73**, 054428 (2006). Nonequilibrium spin currents in this work are considered for free-electron Stoner model for systems with continuously nonuniform magnetization.

¹⁹V. I. Fedorov, A. G. Gukasov, V. Kozlov, S. V. Maleyev, V. P. Plakhty, and I. A. Zokkalo, *Phys. Lett. A* **224**, 372 (1997).

²⁰B. Hu and J. Tekić, *Phys. Rev. Lett.* **87**, 035502 (2001).